SIAM J. APPL. MATH.
Vol. 76, No. 2, pp. 525–550

NONLINEARITY SATURATION AS A SINGULAR PERTURBATION OF THE NONLINEAR SCHRÖDINGER EQUATION*

KARL GLASNER† AND JORDAN ALLEN-FLOWERS†

Abstract. Saturation of a Kerr-type nonlinearity in the nonlinear Schrödinger equation (NLSE) can be regarded as a singular perturbation which regularizes the well-known blow-up phenomenon in the cubic NLSE. An asymptotic expansion is proposed which takes into account multiple scale behavior both in the longitudinal and transverse directions. In one dimension, this leads to a free boundary problem reduction where the solitary wave acts solely to reflect impinging waves and is accelerated by an elastic transfer of momentum. In two dimensions, we find that interaction of a solitary wave and an adjacent wave field is governed by behavior of certain eigenfunctions of the linearized fast-scale operator. This leads to an outer solution with a free logarithmic singularity, whose position evolves by virtue of a large transfer of momentum between the ambient and solitary waves. However, for a certain value of wave power, we find there is essentially no interaction and the solitary wave is asymptotically transparent to the ambient field. We test our results by numerical simulation of both the full equation and free boundary reductions.

Key words. nonlinear Schrödinger equation, multiple scales analysis, singular perturbation

AMS subject classifications. 35Q55, 34E13

DOI. 10.1137/15M1024974

The generalized nonlinear Schrödinger equation (NLSE)

$$i\psi_z + \Delta\psi + F(|\psi|^2)\psi = 0, \quad \psi(\boldsymbol{x}, z) : \mathbb{R}^n \times [0, \infty) \to \mathbb{C} \tag{1}$$

arises in nonlinear optics, fluid dynamics, plasma physics, and Bose–Einstein condensates [45]. It is a generic envelope equation which describes nonlinear propagation of a wave packet whose Fourier components are roughly of a single frequency. The z coordinate describes the direction of propagation (or, in some applications, is the time coordinate), and the Laplacian applies to the transverse coordinates.

The most widely studied version of (1) involves the cubic nonlinearity $F(|\psi|^2)\psi = |\psi|^2\psi$. In one dimension, this equation has a well-known integrable structure [42]. For dimensions $n \geq 2$, it has long been understood [27] that singular behavior of the form $||\psi||_\infty \to \infty$ is possible. This singularity has been analyzed at length [48, 54, 45, 16, 29, 30, 14, 36, 31].

The unphysical nature of singular solutions can be ameliorated by regularizing the equation in a number of ways (see [12] and references therein for a review). For example, the addition of group velocity dispersion leads to temporal pulse splitting and avoids the collapse singularity [10, 32]. Physical effects such as plasma generation may also arrest the singularity [22, 4]. There are also a variety of mathematical treatments which continue the solution past the singularity [35, 34, 15].

Perhaps the most common regularization of (1) involves replacing the cubic nonlinearity with one that saturates at high intensities (see [7] for a review). Wave collapse in this case can lead to the formation of stable solitary waves rather than singularities [47, 33]. The limit of small saturation was studied by Merle [34], who showed that a

*Received by the editors June 9, 2015; accepted for publication (in revised form) December 21, 2015; published electronically March 8, 2016. This work was supported by AFSOR MURI award FA9550-10-1-0561.

http://www.siam.org/journals/siap/76-2/M102497.html

†Department of Mathematics, University of Arizona, Tucson, AZ 85721 (kglasner@math.arizona.edu, jallenf@math.arizona.edu).

weak solution of the cubic NLSE can be obtained past the point of singularity. Our aim is different: we are interested in the approximate behavior of (1) for small but finite saturation terms. This gives rise to rapid variations in all dependent variables, and we introduce an asymptotic expansion which takes this multiple scale behavior into account.

In the optical setting, saturation nonlinearities are often used to describe filamentation, a particular type of robust intense propagation [5, 44, 9, 7, 49]. Individual optical filaments are long-lived, localized waves which exist as a compromise between self-focusing effects and defocusing phenomena. It should be noted that the NLSE is a very rough approximation for ultrashort pulses [7]. In addition, the physical origins and significance of nonlinearity saturation remain controversial [2, 39].

The most conspicuous effect of nonlinearity saturation is the generation of solitary waves (we distinguish these from *solitons*, which are often considered unique to integrable systems), which constitute a family of localized, steadily propagating solutions of (1). Solitary waves of (1) behave somewhat like particles, and by analogy to the quantum mechanical Schrödinger equation are parameterized by quantities like mass, momentum, and position. It is therefore natural to treat solitary waves as coherent structures and study their modulation and interaction.

Modulational theories for one-dimensional solitary waves under various perturbations have been developed previously [26, 25, 8]. Multiple solitary waves may interact by collision or simply through weak communication of the overlap of their far fields [20, 23, 17]. A general purpose perturbation scheme for the latter [20, 23, 11] yields ordinary differential equations (ODEs) which describe cross-modulation of the underlying solitary wave parameters. Because of the Hamiltonian structure of the problem, there is an equivalent variational method for solitary wave interaction, which involves an expansion of the Hamiltonian functional by assuming some wave field ansatz. This has been used in the optical context to describe interaction of multiple localized beams [6, 5, 52]. The particle analogy has been further carried out to describe merging, annihilation, and nucleation of solitary wave structures [43, 28].

Long-range communication of solitary waves in the NLSE is generally very weak because it arises from an exponentially small mismatch in the tails of the wave profiles. Nonlocal mechanisms such as steady state heat transfer or material elasticity (in liquid crystals, for example) can alter this picture, however, and lead to significant interaction [40, 1].

Because wave dispersion can be a relatively slow effect, solitary waves often exist within an ambient wave field which may contain significant power despite being of modest amplitude. This has been noted, for example, in optical filamentation [7]. In principle, this means that interaction between solitary waves and an ambient field might occur. A quantification of this effect is therefore desirable.

What the effect of a small perturbative wave field might be is of course a natural question when discussing orbital stability of solitary waves. Considerable progress has been made in the direction of rigorous analysis (see [46] for a review). A major aspect of the stability calculation involves determining modulation equations, which are ODEs that describe the evolution of wave parameters as a function of the perturbation (see, e.g., [51]). Apart from stability, control of solitary wave structures is often of practical interest [13], which requires understanding the role of perturbative forcing.

In many applications, solitary waves have high intensities and involve length- and timescales much smaller than the ambient waves that surround them. This poses considerable practical difficulty in direct numerical simulations [44, 9], which must re-

solve these scales adequately. It is therefore natural to seek a reduced set of equations which have the small scales removed.

This paper uses multiple scale analysis and asymptotic matching techniques, as well as numerical experiments, to study the effect of a singular perturbation induced by small nonlinearity saturation. We have two aims in doing this. The first is to consider the "scattering" effect of a high-intensity solitary wave on an ambient, slowly varying wave field of modest intensity. The second is the opposite: we ask if high-intensity solitary waves are modulated in the presence of an external wave field.

We find that the interaction of solitary and ambient waves are governed primarily by an eigenfunction which arises from linearization about the solitary wave. For one transverse dimension, the eigenfunction grows linearly in the far field, which by matching provides a reflective boundary condition and a slow-scale transfer of momentum. In two dimensions, the relevant eigenfunction may or may not grow logarithmically, and this difference leads to qualitatively different scenarios. In the logarithmic case, an expansion which accommodates singular behavior in the outer solution is sought, which is coupled to the motion of the singularity by transfer of momentum between the solitary and ambient waves.

The paper is organized as follows. Some basic properties of the nonlinear Schrödinger equation are reviewed in section 1. In section 2 we introduce the singular perturbation and the expansion which we use. The case of one transverse dimension is discussed in section 3, wherein a free boundary reduction is obtained and verified numerically. Section 4 discusses the case of two transverse dimensions. A free singularity problem is derived and compared to the full evolution equation (1) numerically.

1. Properties of the generalized nonlinear Schrödinger equation. The literature on mathematical aspects of (1) is extensive (see, e.g., [45]). Our work will specialize to a class of nonlinearities $F(|\psi|^2) = |\psi|^2 - \gamma|\psi|^{2K}$ with $K > 1$. It has been shown that under broad circumstances this type of regularization is sufficient for global (in z) well-posedness [18, 24, 34]. Some of the other properties of (1) which will be required are reviewed below.

1.1. Conservation and symmetry. By analogy to the quantum mechanical interpretation, equation (1) has several conserved quantities. The most relevant here are power I and momentum $\mathbf{\Pi}$,

$$I = \int |\psi|^2 d\boldsymbol{x}, \quad \mathbf{\Pi} = 2\mathrm{Im} \int \psi^* \nabla\psi d\boldsymbol{x}, \tag{2}$$

where throughout integrals are over $\mathbb{R}^n$ unless otherwise specified. In particular, the power and momentum densities obey the conservation laws

$$(|\psi|^2)_z + \nabla\cdot\boldsymbol{j} = 0, \quad (2\mathrm{Im}\psi^*\nabla\psi)_z + \nabla\cdot\boldsymbol{T} = 0, \tag{3}$$

where the power flux is

$$\boldsymbol{j} = -2\mathrm{Im}\psi\nabla\psi^* \tag{4}$$

and the (quantum mechanical) stress tensor is

$$\boldsymbol{T} = -\Delta(|\psi|^2)\mathbf{Id} + 4\mathrm{Re}(\nabla\psi\otimes\nabla\psi^*) + G(|\psi|^2)\mathbf{Id}, \tag{5}$$

where $\mathbf{Id}$ is the identity tensor and $G(|\psi|^2) = -2[F(|\psi|^2)|\psi|^2 - \Phi(|\psi|^2)]$ with $\Phi' \equiv F$. It follows that if ψ decays sufficiently fast as $|\boldsymbol{x}| \to \infty$, then $dI/dz = 0$ and $d\mathbf{\Pi}/dz = 0$.

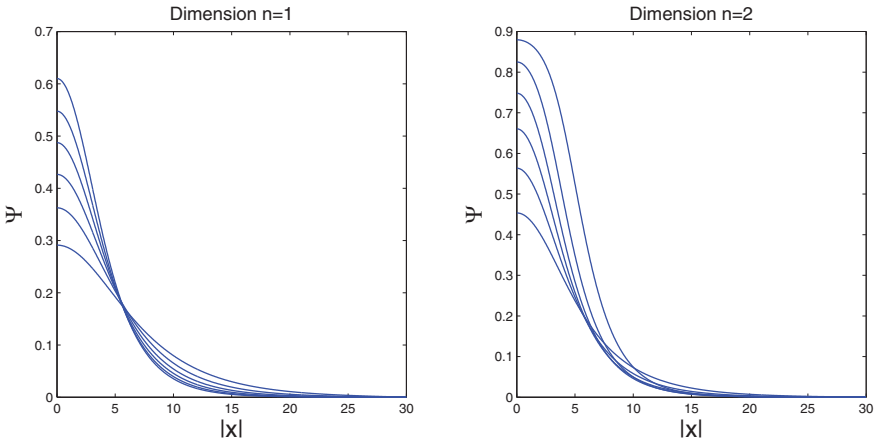

FIG. 1. *Solitary wave profiles solving* (7) *in dimensions* $n = 1, 2$. *Each plot has* $\Lambda = 0.04, 0.06, 0.08, 0.1, 0.12, 0.14$, *where the amplitude increases with* Λ.

Another useful property concerns symmetry of the NLSE (1) under Galilean transformations. This asserts that if $\psi(\boldsymbol{x}, z)$ is a solution, so is

$$\psi'(\boldsymbol{x}, z) = \exp(i\boldsymbol{v}_0[\boldsymbol{x}/2 - z/4])\psi(\boldsymbol{x} - \boldsymbol{v}_0 z, z), \tag{6}$$

where $\boldsymbol{v}_0$ represents the velocity of a moving reference frame.

1.2. Solitary waves. Equation (1) admits solitary waves of the form $\psi = \exp(i\Lambda z)\Psi(\boldsymbol{x}; \Lambda)$, where the real-valued intensity profile Ψ satisfies

$$\Delta\Psi - \Lambda\Psi + F(|\Psi|^2)\Psi = 0, \quad \lim_{\boldsymbol{x}\to\infty} \Psi(\boldsymbol{x}) = 0. \tag{7}$$

Properties of this equation are well established (see, e.g., [3]). In particular, it has been shown that solutions of (7) are necessarily radially symmetric [45]. Of course, in general, the NLSE has a variety of nonsymmetric solutions (see, e.g., [53]).

For dimension $n = 1$ and specific nonlinearity

$$F(|\psi|^2) = |\psi|^2 - |\psi|^4, \tag{8}$$

solutions of (7) can be found explicitly [47] and comprise a continuous family

$$\Psi(x; \Lambda) = \left(\frac{12\Lambda}{\sqrt{9 - 48\Lambda}\cosh(2\sqrt{\Lambda}x) + 3} \right)^{\frac{1}{2}} \tag{9}$$

for $0 < \Lambda < 3/16$. For $n = 2$ solutions must be obtained numerically, but there is still a continuous family for $0 < \Lambda < \Lambda_{max}$ where $\Lambda_{max} \approx 0.15$. Figure 1 shows the profiles (7) for dimensions $n = 1$ and $n = 2$.

Due to the Galilean and other symmetries of (1), a more general class of solitary waves can be formed:

$$\psi_{sol}(\boldsymbol{x}, z; \Lambda, \boldsymbol{x}_0, \boldsymbol{v}, \alpha) = \exp\left(i\Lambda z + i\boldsymbol{v} \cdot [\boldsymbol{x}/2 - z\boldsymbol{v}/4] + \alpha z\right)\Psi(\boldsymbol{x} - \boldsymbol{x}_0 - z\boldsymbol{v}; \Lambda). \tag{10}$$

In dimensions $n = 1$ and $n = 2$, there is a one-to-one correspondence between the parameters $\Lambda, \boldsymbol{v}$ and the conserved quantities I and $\boldsymbol{\Pi}$. In particular the power (mass)

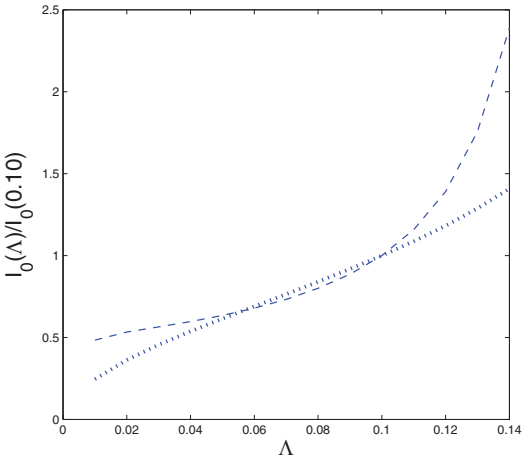

FIG. 2. *Solitary wave power for dimension $n = 1$ (dotted) and $n = 2$ (dashed), scaled for easy visualization. The Vakhitov–Kolokolov criteria* [47] $dI_0/d\Lambda > 0$ *is met in both cases.*

of the solitary wave is a function of Λ alone,

$$I_0(\Lambda) = \int |\Psi(\boldsymbol{x}; \Lambda)|^2 \, d\boldsymbol{x}, \tag{11}$$

and the momentum is a function of $\boldsymbol{v}$ and Λ,

$$\boldsymbol{\Pi}_0(\Lambda, \boldsymbol{v}) = \boldsymbol{v} \int |\Psi(\boldsymbol{x}; \Lambda)|^2 \, d\boldsymbol{x} = \boldsymbol{v} I_0(\Lambda). \tag{12}$$

1.3. Stability of solitary waves. Solitary waves of the form (10) often occur for a wide variety of initial conditions and may possess a strongly stabilizing property. Stability (in the orbital sense) can be analyzed by perturbing $\psi = \psi_{sol} + \exp(-i\Omega z + i\Lambda z)\psi'(x)$ to obtain a linear problem for ψ' which has been studied at length. It turns out that there exists at most one eigenvalue Ω with nonzero imaginary part [21, 37]. In addition, if the Vakhitov–Kolokolov criterion $dI_0/d\Lambda > 0$ is met [47], there are no such eigenvalues. Figure 2 shows the dependence of the power I_0 on Λ for the particular nonlinearity (8).

Although we limit our study to the case where there are only stable solitary waves, long-lived neutral modes can sometimes play a role in the nonlinear setting. Bound eigenfunctions for $|\Omega| < \Lambda$, often called internal modes [38], may also be present, but there is a large range in Λ where no such bound states occur [44]. Unlike continuous modes which rapidly disperse away, internal modes persist and only decay because of nonlinear harmonic generation, which transfers energy to the dispersive part of the spectrum.

2. Saturation of the nonlinearity as a singular perturbation. As explained in the introduction, there is a great practical need to understand the role of high-intensity solitary waves and ameliorate the difficulty associated with the small scales they introduce. This section develops a framework which exploits a separation of scales using a combination of matched and multiple scale asymptotics.

To investigate the role of saturation of the nonlinearity in (1), we consider nonlinearities of the form $F(|\psi|^2) = |\psi|^2 - \gamma|\psi|^{2K}$ with $K > 1$ an integer (expressions such as these arise, for example, in modeling multiphoton ionization [44]). The basic idea here is to regard the term $\gamma|\psi|^{2K}\psi$ as a singular perturbation of the cubic NLSE.

The problem can be made suitable for an asymptotic expansion by writing the the nonlinear term as

$$F(|\psi|^2)\psi = \epsilon^{-2} f(\epsilon^2|\psi|^2)\psi, \quad f(U^2) \equiv U^2 - U^{2K}, \quad \epsilon = (\gamma)^{1/(2K-2)} \ll 1. \tag{13}$$

For this particular class of nonlinearities, the family of (high-intensity) solitary waves can be written

$$\psi_{sol} = \epsilon^{-1} \exp(i\lambda z/\epsilon^2 + i\boldsymbol{v} \cdot [\epsilon\boldsymbol{\xi}/2 + z\boldsymbol{v}/4] + i\alpha) U(|\boldsymbol{\xi}|; \lambda), \quad \boldsymbol{\xi} = [\boldsymbol{x} - z\boldsymbol{v}]/\epsilon, \tag{14}$$

where the radial profile $U(r, \lambda)$ satisfies

$$\frac{1}{r^2}U'' + \frac{n-1}{r}U' - \lambda U + f(|U|^2)U = 0, \quad \lim_{r\to\infty} U = 0, \tag{15}$$

and the scaled parameter is $\lambda = \epsilon^2\Lambda$. The effect of the singular perturbation on solitary waves by themselves is clear. Provided $\lambda = O(1)$, they are narrow, rapidly oscillating structures with large amplitude.

2.1. A hybrid matched/multiple scale expansion. If a solitary wave (or many of them) is combined with a small amplitude wave field, a modulation of the solitary wave via nonlinear interaction might be expected. Conversely, the solitary wave may act as a reflector or source for the wave field. These effects will be quantified by a combination of multiple scale techniques.

We suppose that away from the solitary wave, where $|\boldsymbol{\xi}| \gg 1$, ψ and its derivatives are $O(1)$. In dimension $n = 1$ and a special case for dimension $n = 2$, the outer solution can be simply expanded powers

$$\psi = \psi_0 + \epsilon\psi_1 + O(\epsilon^2), \quad \epsilon \to 0. \tag{16}$$

The general two-dimensional case requires a special treatment because of the necessity to match logarithmically growing terms in the inner expansion. Details are given in section 4.2.

It might be expected that the modulation of the solitary wave, via evolution of the wave parameters, occurs on some slow scale $Z = \alpha(\epsilon)z$ with $\alpha(\epsilon)$ to be determined. By virtue of (14) there is also a fast scale for oscillations, which is accounted for by introducing the phase variable $\theta = \epsilon^{-2}\alpha(\epsilon)^{-1}\phi(Z)$. This phase variable is equivalent to the exponential factor in a WKB-type expansion, and is calibrated by the assumption that u is 2π-periodic in θ. The slowly varying factor $\phi(Z)$ is needed to accommodate a potential modulation effect that would result from evolution of λ. The inner spatial coordinate is $\boldsymbol{\xi} = [\boldsymbol{x} - \boldsymbol{x}_0(z, Z)]/\epsilon$, where the Z dependence accounts for the possible acceleration by modulation of momentum.

The inner solution, valid where $|\boldsymbol{\xi}| \ll \epsilon^{-1}$, will be labeled $u = u(\boldsymbol{\xi}, \theta, z, Z)$, so that (1) becomes

$$i\phi' u_\theta + \epsilon^2 i u_z + \epsilon^2\alpha(\epsilon) i u_Z - \epsilon\alpha(\epsilon) i\boldsymbol{v} \cdot \nabla u + \Delta u + F(|u|^2)u = 0, \tag{17}$$

where $\boldsymbol{v} = [\partial_z + \alpha(\epsilon)\partial_Z]\boldsymbol{x}_0$ and the spatial operators are with respect to $\boldsymbol{\xi}$. In one dimension and the two-dimensional special case (section 4.1), u is expanded:

$$u \sim \epsilon^{-1}u_0 + u_1 + \epsilon u_2 + \epsilon^2 u_3 + O(\epsilon^4), \quad \epsilon \to 0. \tag{18}$$

The more general two-dimensional case will be expanded as follows:

$$u \sim \epsilon^{-1}u_0 + u_1 + \chi(\epsilon)u_\dagger + \epsilon u_2 + \epsilon\chi(\epsilon)^2 u_{\dagger\dagger} + \epsilon\chi(\epsilon)^3 u_{\dagger\dagger\dagger} + O(\epsilon^3), \tag{19}$$

where the order function $\chi(\epsilon)$ has the property $\chi(\epsilon)^k \gg \epsilon$ for $k \geq 1$ and will be determined by matching (see section 4.2).

2.2. Modulation of solitary wave parameters. One goal of the approximation procedure is to extract the slow-scale dynamics $d\lambda/dZ$, $d\boldsymbol{v}/dZ$. Although these terms eventually appear explicitly in the expansion of (17) (at orders $\alpha(\epsilon)\epsilon^2$ and $\alpha(\epsilon)\epsilon^3$, respectively), it is both more lucid and tractable to expand (3) directly. Since the wave parameter λ and the scaled leading order power $I_0(\lambda)$ are in one-to-one correspondence, modulation of λ can be achieved by flux of power from the inner to the outer solution. Similarly, the solitary wave velocity can be related to flux of both power and momentum.

For later use, we record the conservation laws (3) written in terms of the inner expansion variables. In the moving frame of reference, the expression for power density flux becomes

$$D_z|u|^2 + \epsilon^{-1}\nabla\cdot\boldsymbol{j}_m = 0, \quad \boldsymbol{j}_m \equiv -2\epsilon^{-1}\mathrm{Im}[u\nabla u^*] - \boldsymbol{v}|u|^2, \tag{20}$$

where $D_z \equiv \partial/\partial z + \alpha(\epsilon)\partial/\partial Z + \epsilon^{-2}\phi'\partial/\partial\theta$. The momentum density flux becomes

$$D_z(2\mathrm{Im}[u^*\nabla u]) + \nabla\cdot\boldsymbol{T}_m = 0, \tag{21}$$

where

$$\boldsymbol{T}_m \equiv -\epsilon^{-2}\Delta(|u|^2)\mathbf{Id} + 4\epsilon^{-2}\mathrm{Re}(\nabla u\otimes\nabla u^*) + G(|u|^2)\mathbf{Id} - 2\epsilon^{-1}\mathrm{Im}[u^*\nabla u]\otimes\boldsymbol{v}.$$

Integration of (20) and (21) over a disk of radius r gives (using the divergence theorem)

$$D_z\int_{|\boldsymbol{\xi}|<r}|u|^2 d\boldsymbol{\xi} = -\epsilon^{-1}\int_{|\boldsymbol{\xi}|=r}\boldsymbol{j}_m\cdot\boldsymbol{n}\,d\boldsymbol{\xi} \tag{22}$$

and

$$D_z\int_{|\boldsymbol{\xi}|<r}2\mathrm{Im}[u^*\nabla u]d\boldsymbol{\xi} = -\int_{|\boldsymbol{\xi}|=r}\boldsymbol{T}_m\cdot\boldsymbol{n}\,d\boldsymbol{\xi}. \tag{23}$$

As is always assumed in asymptotic matching, we suppose that $r = |\boldsymbol{\xi}|$ can be taken to ∞ at the same time as $\epsilon \to 0$, in such a way as to leave only the leading order terms on each side of these expressions. For purposes of clarity, this double asymptotic limit will be denoted $\epsilon \to 0$, $r \to \infty$.

2.3. Form of the expansion equations. The leading order term u_0 is a solution to the unperturbed equation (the $O(\epsilon^{-1})$ terms in (17))

$$i\phi'(Z)u_{0\theta} + \Delta u_0 + f(|u_0|^2)u_0 = 0. \tag{24}$$

By the assumption that u is periodic in θ, u_0 may be an unperturbed solitary wave

$$u_0 = e^{i\theta + i\Theta}U(\boldsymbol{\xi};\lambda), \tag{25}$$

where $\Theta = \Theta(z)$ is the slowly evolving part of the phase, which is needed to accommodate the velocity-dependent phase term in (14). The fast phase variable is then recovered from integrating $\phi'(Z) = \lambda(Z)$.

There is a subtle technical issue which arises from ambiguities in the leading order solution. In (25), the introduction of λ is not well defined, since replacing λ with $\lambda+\epsilon\lambda'$ would yield an equally valid leading order solution $u_0' = e^{i\theta+i\Theta}U(\boldsymbol{\xi};\lambda+\epsilon\lambda')$. This differs by an $O(\epsilon)$ quantity from the original, and this difference would be incorporated into higher terms in the expansion; for example, u_1 would be modified by an amount $-\lambda' e^{i\theta+i\Theta}U_\lambda$, which is the $O(\epsilon)$ term in the difference of $u_0' - u_0$. To eliminate this ambiguity, the parameter λ is defined (for a given solution family $\psi = \psi(\cdot;\epsilon)$) so as to eliminate the U_λ component from all correction terms by the orthogonality condition

$$\text{Re}\int_0^{2\pi}\int e^{i\theta}U_\lambda u_j^*\, d\boldsymbol{\xi}d\theta = 0, \quad j = 1,2,3,\ldots. \tag{26}$$

In a similar vein, the phase variable Θ and inner coordinate $\boldsymbol{\xi}$ can be uniquely defined if one assumes the orthogonality relations

$$\text{Im}\int_0^{2\pi}\int e^{i\theta}U\, u_j^*\, d\boldsymbol{\xi}d\theta = 0, \quad j = 1,2,3,\ldots, \tag{27}$$

and

$$\text{Re}\int_0^{2\pi}\int e^{i\theta}\nabla U\, u_j^*\, d\boldsymbol{\xi}d\theta = \mathbf{0}, \quad j = 1,2,3,\ldots, \tag{28}$$

which eliminate the phase and translation symmetries.

The remaining expansion terms have the form $\mathcal{L}u_n = e^{i\Theta}R_n$, where the linear operator

$$\mathcal{L}\eta \equiv i\lambda\eta_\theta + \Delta\eta + [f(U^2) + U^2 f'(U^2)]\eta + e^{2i[\theta+\Theta]}U^2 f'(U^2)\eta^* \tag{29}$$

acts on functions of θ and $\boldsymbol{\xi}$. By periodicity in θ, one can Fourier expand η and the right-hand sides R_n as

$$\eta = e^{i\Theta}\sum_{-\infty}^{\infty}\hat{\eta}(\boldsymbol{\xi},k,z,Z)e^{ik\theta}, \quad R_n = \sum_{-\infty}^{\infty}\hat{R}_n(\boldsymbol{\xi},k,z,Z)e^{ik\theta}, \tag{30}$$

which decomposes the operator into components having the form

$$-k\lambda\eta_k + \Delta\eta_k + [f(U^2) + U^2 f'(U^2)]\eta_k + U^2 f'(U^2)\eta_{2-k}^* = \hat{R}(\boldsymbol{\xi},k,\cdot), \tag{31}$$

where for notational convenience $\eta_k = \hat{\eta}(\boldsymbol{\xi},k,\cdot)$. For $k \neq 1$, the k and $2-k$ modes are coupled in a pairwise fashion, whereas the $k = 1$ mode is uncoupled. We note that (31) is linear only for the real and imaginary parts separately. It is also useful to observe that the linear operator acting on (the real or imaginary parts of) the coupled subsystem for η_k and η_{2-k} is self-adjoint with respect to the inner product

$$\langle[\eta_k\ \eta_{2-k}],[\eta_k'\ \eta_{2-k}']\rangle = \int \eta_k\eta_k' + \eta_{2-k}\eta_{2-k}'\, d\boldsymbol{\xi}. \tag{32}$$

2.4. Nullspace of the linearized operator. In order to implement both Fredholm-type conditions as well as asymptotic matching, a detailed study of the operator $\mathcal{L}$ is required. Since the outer solution ψ by assumption does not have rapid oscillations, $\mathcal{L}$ is regarded here as acting on sufficiently smooth functions $\eta : \mathbb{R}^n \times [0,2\pi) \to \mathbb{C}$ which are 2π-periodic in θ and whose Fourier components satisfy

$$\lim_{|\boldsymbol{\xi}|\to\infty}\hat{\eta}(\boldsymbol{\xi},k) = 0, \quad k \neq 0. \tag{33}$$

On the other hand, standard matching conditions (e.g., (49)) in general require logarithmic or polynomial growth in the nonoscillating component $\hat{\eta}(\boldsymbol{\xi}, 0)$. By virtue of the decomposition (31), the kernel of $\mathcal{L}$ can be studied by looking at each coupled subsystem separately.

For $k = 1$, writing the complex Fourier component $\eta_1 = \nu + i\mu$, the corresponding nullspace components solve

$$-\lambda\nu + \Delta\nu + [f(U^2) + 2U^2 f'(U^2)]\nu = 0, \tag{34}$$

$$-\lambda\mu + \Delta\mu + f(U^2)\mu = 0. \tag{35}$$

Regarding the solution $U = U(|\boldsymbol{\xi}|)$ of (15) as a function of $\boldsymbol{\xi}$, spatial differentiation of this equation gives solutions of (34) as $\nu = \nabla U(|\boldsymbol{\xi}|)$. The second equation (35) is in fact the same as the one for the solitary wave profile (15). It follows that the nullspace of $\mathcal{L}$ has "symmetry" eigenmodes

$$\eta_p = iUe^{i\theta}, \quad \eta_x = U_x e^{i\theta}, \quad \eta_y = U_y e^{i\theta}, \tag{36}$$

which correspond to symmetries of the underlying equation.

The coupling of the $k = 0$ and $k = 2$ Fourier components give rise to a system involving η_0 and η_2. Decomposing $(\eta_0, \eta_2) = (\nu_0 + i\mu_0, \nu_2 + i\mu_2)$, it follows that the corresponding nullspace components solve

$$\Delta\nu_0 + [f(U^2) + U^2 f'(U^2)]\nu_0 + U^2 f'(U^2)\nu_2 = 0, \tag{37}$$

$$\Delta\nu_2 - 2\lambda\nu_2 + [f(U^2) + U^2 f'(U^2)]\nu_2 + U^2 f'(U^2)\nu_0 = 0, \tag{38}$$

and

$$\Delta\mu_0 + [f(U^2) + U^2 f'(U^2)]\mu_0 - U^2 f'(U^2)\mu_2 = 0, \tag{39}$$

$$\Delta\mu_2 - 2\lambda\mu_2 + [f(U^2) + U^2 f'(U^2)]\mu_2 - U^2 f'(U^2)\mu_0 = 0, \tag{40}$$

subject to boundary conditions $\lim_{|\boldsymbol{\xi}|\to\infty}(\nu_2 + i\mu_2) = 0$. Note that any solution (ν_0, ν_2) to (37)–(38) means that $(\mu_0, \mu_2) = (\nu_0, -\nu_2)$ is a solution to (39)–(40). In terms of the original operator, it follows that the nullspace has elements

$$\eta_{i\pm} = \nu_0(\boldsymbol{\xi}) \pm e^{2i\theta}\nu_2(\boldsymbol{\xi}), \tag{41}$$

which will be called "interaction modes," since they are responsible for transmitting asymptotic matching information between the solitary wave and outer solution wave field.

For dimension $n = 1$, the system (37)–(38) has a pair of linearly independent solutions $(\nu_0, \nu_2) = (P, Q)$ and $(\nu_0, \nu_2) = (\tilde{P}, \tilde{Q})$. These can be chosen so that (P, Q) has even symmetry in $\boldsymbol{\xi}$ and $[\tilde{P}, \tilde{Q}]$ has odd symmetry (Figure 3). Some of these solutions have been computed numerically for the nonlinearity (8) using an elementary shooting method and are shown in Figure 3.

In two dimensions, the solutions of (37)–(38) can be sought by separating variables in coordinates (r, φ), where $r = |\boldsymbol{\xi}|$ and φ is the polar angle. For $(\nu_0, \nu_2) = \cos(m\varphi)\big(P_m(r), Q_m(r)\big)$, $m = 0, 1, 2, \ldots$, this leads to

$$\frac{1}{r}(rP_m')' - \frac{m^2}{r^2}P_m + [f(U^2) + U^2 f'(U^2)]P_m + U^2 f'(U^2)Q_m = 0, \tag{42}$$

$$\frac{1}{r}(rQ_m')' - \frac{m^2}{r^2}Q_m - 2\lambda Q_m + [f(U^2) + U^2 f'(U^2)]Q_m + U^2 f'(U^2)P_m = 0. \tag{43}$$

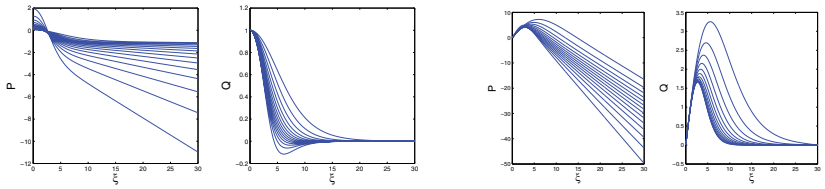

(a) Odd eigenfunctions (b) Even eigenfunctions

FIG. 3. *Even (left) and odd (right) solutions of* (37)–(38) *in one dimension. In increasing value near* $\xi = 0$*, plots correspond to* $\lambda = 0.01, 0.02, \ldots, 0.15$.

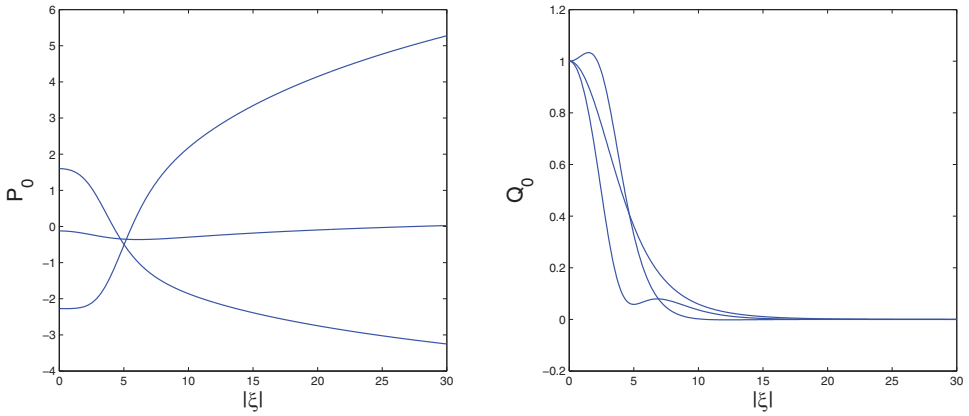

FIG. 4. *Solutions of* (42)–(43) *for* $m = 0$ *and* $\lambda = 0.04, 0.10, 0.13$*, where both* P_0 *and* Q_0 *are decreasing near* $\xi = 0$ *as a function of* λ.

Purely radial solutions with $m = 0$ can be found by imposing $P_0'(0) = 0 = Q_0'(0)$ and $Q_0(\infty) = 0$, where the former conditions are required by smoothness at the origin. A shooting method similar to the one-dimensional case was used to find these solutions (Figure 4). For $m = 1$, smoothness of solutions of (37)–(38) at the origin require $P_1(0) = 0 = Q_1(0)$ instead; computations of these are given in Figure 5. While it is possible to find modes for $m \geq 2$, these are not required in what follows.

Matching to the outer wave field will require the $\boldsymbol{\xi} \to \infty$ asymptotics of the nullspace eigenfunctions. In one dimension, as $|\xi| \to \infty$ both $P, \tilde{P}$ satisfy $\nu_0'' \sim 0$, and as a consequence the far-field behavior is simply linear. For two dimensions, one has

$$r(rP_m')' - m^2 P_m \sim 0, \quad r \to \infty,$$

which generically leads to the behavior $P_m \sim r^m$ if $m \geq 1$ and logarithmic behavior for $m = 0$. For one-dimensional and radially symmetric ($m = 0$) eigenfunctions, the far-field behavior can therefore be written as

$$\nu_0 \sim \begin{cases} a(\lambda) + m(\lambda)|\xi|, & n = 1, \\ a(\lambda) + m(\lambda) \ln |\boldsymbol{\xi}|, & n = 2, \end{cases} \qquad \boldsymbol{\xi} \to \infty, \tag{44}$$

where the coefficients a and m are unique up to scaling. We have computed the ratio $m(\lambda)/a(\lambda)$ in the case of nonlinearity (8) for various values of λ (Figure 6). In two dimensions, there are two qualitative features of note. The first is that for $\lambda \approx 0.077$,

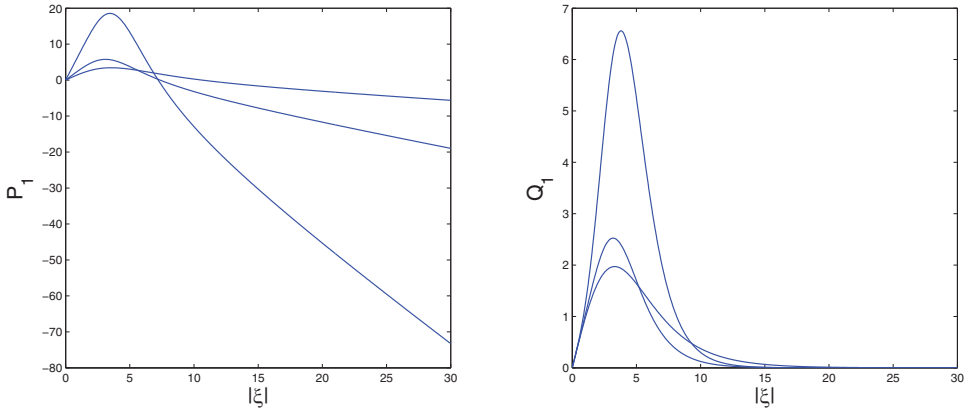

FIG. 5. *Solutions of* (42)–(43) *for* $m = 1$ *and* $\lambda = 0.04, 0.10, 0.13$, *where both* P_1 *and* Q_1 *are increasing near* $\xi = 0$ *as a function of* λ.

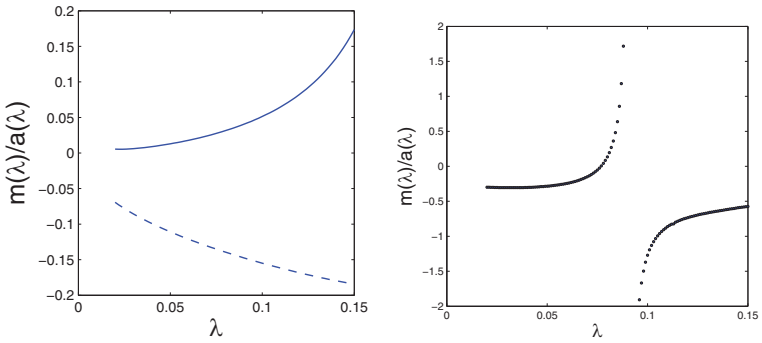

(a) dimension $n = 1$ (b) dimension $n = 2$

FIG. 6. *Dependence of asymptotic behavior* (44) *on* λ *in one (left) and two (right) dimensions. For dimension* $n = 1$, *the solid line corresponds to the even eigenfunction component* P, *and the dashed line corresponds to the odd component* $\tilde{P}$.

there is no logarithmic far-field behavior; this allows us to ignore logarithmic terms in the expansion. In contrast, when $\lambda \approx 0.092$, the far-field behavior has $a = 0$. In one dimension, both the odd and even eigenfunction components $P, \tilde{P}$ have a nonzero ratio of m/a. This will have strong implications for matching to the outer solution.

3. Dimension $n = 1$. We now specialize to the case of one transverse dimension. The goal is to find a free boundary problem satisfied by the outer solution. This has the effect of analytically eliminating the small scales present in the rapidly oscillating solitary wave, while retaining information about the wave parameters.

The correction term at order ϵ in (17) is

$$\mathcal{L}u_1 = -ivU_\xi e^{i[\theta+\Theta]}. \tag{45}$$

The most general solution which incorporates possible nullspace components is

$$u_1 = e^{i\Theta}\Big\{AP + A^*Qe^{2i\theta} + \tilde{A}\tilde{P} + \tilde{A}^*\tilde{Q}e^{2i\theta} + iU\big[\beta + v\xi/2\big]e^{i\theta} + \mu U_\xi e^{i\theta}\Big\}, \tag{46}$$

where, using the orthogonality relations (27), (28), the constants $\beta, \mu = 0$. Since both

$P, \tilde{P}$ have linear growth for large $|\xi|$, these terms cannot be matched to the outer solution. It follows that $A = 0 = \tilde{A}$, and by matching to the value of the outer solution one obtains a free boundary condition $\psi_0(x_0) = 0$. To leading order, the ambient wave will therefore be reflected off of the solitary wave.

The next order equation is $\mathcal{L}u_2 = e^{i\Theta}R_2$, where

$$-R_2 = \left[(v\xi/2)^2 U^3 f'(U^2) - \Theta_z U\right] e^{i\theta} - \frac{1}{2} v[v\xi U]_\xi. \tag{47}$$

This equation admits a particular solution:

$$u_{2part} = \Big[-\frac{1}{8}(v\xi)^2 U + (\Theta_z - v^2/4)U_\lambda \Big] e^{i\theta}. \tag{48}$$

Notice that imposing the orthogonality condition (26) recovers the slow variation in phase $\Theta_z = v^2/4$ in the unperturbed moving solitary wave (14). The remaining part of the solution for u_2 involves nullspace terms as in (46). In particular, since both $P, \tilde{P}$ have linear behavior in the far field, there is necessarily a superposition of these which accommodates matching to the outer solution, which requires

$$u_2 \sim \begin{cases} \psi_{0x}(x_0^+)\xi, & \xi \to \infty, \\ \psi_{0x}(x_0^-)\xi, & \xi \to -\infty, \end{cases} \tag{49}$$

where $x_0^\pm$ refers to limits from the left $(-)$ and right $(+)$.

The modulation of solitary wave parameters can now be computed using (22) and (23). Applying the double limit $\epsilon \to 0$, $r \to \infty$, the power and (scalar) momentum of the inner solution in (22), (23) are to leading order

$$\epsilon^{-1} \int U(\xi;\lambda)^2 \, d\xi = \epsilon^{-1} I_0(\lambda), \quad \epsilon^{-1} v \int U(\xi;\lambda)^2 \, d\xi = \epsilon^{-1} \mathbf{\Pi}_0(\lambda, v), \tag{50}$$

respectively. The (scalar) momentum flux (21) is $T_m \sim 2|u_{2x}|^2$ for $\epsilon \to 0, |\xi| \to \infty$. With the choice of slow scale $\alpha(\epsilon) = \epsilon$, the leading order momentum balance (22) can be found using (49), giving

$$d\mathbf{\Pi}_0/dZ = 2\Big(|\psi_{0x}(x_0^-)|^2 - |\psi_{0x}(x_0^+)|^2 \Big), \quad \epsilon \to 0. \tag{51}$$

This means that an ambient wave will transfer momentum to the solitary wave analogous to an elastic collision. On the other hand, by virtue of the fact that u_1 is exponentially decaying, the leading order power flux is $\boldsymbol{j}_m \sim -2\epsilon \mathrm{Im}[u_2 u_{2\xi}]$ for $\epsilon \to 0, |\xi| \to \infty$. In principle this could be evaluated by higher order matching to the outer solution, but it is enough to observe that power modulation is $dI_0/dz = O(\epsilon^2)$, which is slower by a factor of ϵ than momentum transfer.

In summary, the leading order problem for $\psi \approx \psi_0$ satisfies a free boundary problem

$$\begin{aligned} i\psi_z + \psi_{xx} + |\psi|^2\psi = 0, \quad x \neq x_0(z), \quad \psi(x_0(z), z) = 0, \\ \frac{d^2 x_0}{dz^2} = \frac{2\epsilon}{I_0(\lambda)} \Big(|\psi_x(x_0^-)|^2 - |\psi_x(x_0^+)|^2 \Big). \end{aligned} \tag{52}$$

3.1. Numerical verification. We now compare the full and reduced model equations using numerical computations. The numerical methods employed for (1) are a modification of a well-known conservative scheme [41], whose details are given in Appendix A.

The free boundary problem (52) can be reformulated so that the free boundary is no longer dynamic. By a change of variables $y = x - x_0(z)$, $\tilde{\psi}(y,t) = \psi(y + x_0(z), z)$ satisfies

$$
\begin{aligned}
(53) \qquad i[\tilde{\psi}_z - v(z)\tilde{\psi}_y] + \tilde{\psi}_{yy} + |\tilde{\psi}|^2\tilde{\psi} = 0, \quad y \neq 0,\\
\tilde{\psi}(0,z) = 0,\\
v_z = \frac{2\epsilon}{I_0(\lambda)}\Big(|\tilde{\psi}_y(0^-)|^2 - |\tilde{\psi}_y(0^+)|^2\Big).
\end{aligned}
$$

This problem can be solved numerically in each subdomain $(-\infty, 0)$, $(0, \infty)$ separately, with $v(z)$ updated at each timestep.

To compare the free boundary reduction to the original NLSE (1), the initial conditions for (53) were chosen to represent an initially stationary solitary wave at zero and an ambient wave field with a modulated Gaussian profile

$$
v(0) = 0, \quad \tilde{\psi}(y,0) = w(y), \quad w(x) = \exp(-(x - x_c)^2 + iv_g(x - x_c)/2).
$$

For the singularly perturbed equation (1) with the cubic-quintic nonlinearity (8), the initial condition was the same except a solitary wave was added:

$$
\psi(x,0) = \epsilon^{-1}U\left(\frac{x}{\epsilon};\lambda\right) + w(x),
$$

where $\lambda = 0.08$. To ensure that the Gaussian profile interacts with the solitary wave, it is initially centered at $x_c = -5$ with $v_g = 2$. Both simulations were conducted on an interval $[-15, 15]$ using Neumann boundary conditions.

The solitary wave position $x_0(z)$ was computed for both (1) and (53). In the latter case this was obtained by integrating $v(z)$. Figure 7 shows the evolution of this quantity for several different values of ϵ. In general, the two models have improving agreement as ϵ is decreased. The difference between the outer solutions was also computed, defined as the L_1 norm of the difference on a set excluding the solitary wave region $I = (-15, 15)/(\boldsymbol{x}_0 - 10\epsilon, \boldsymbol{x}_0 + 10\epsilon)$,

$$
L_1 \text{ Error} = \int_I |\tilde{\psi} - \psi|\, dx.
$$

Figure 8 shows the evolution of this quantity. Again, the agreement between the two models improves with decreasing ϵ.

4. Dimension $n = 2$. In two dimensions, it was observed that the behavior of the eigenfunction component P_0 can be either constant or logarithmic in the far field, depending on the parameter λ. We separate these two cases to emphasize the qualitative difference between them.

4.1. Expansion for $m(\lambda) = 0$. In this case, the regular expansion (18) is sufficient. The second expansion equation ($O(\epsilon^0)$ terms in (17)) reads

$$
(54) \qquad \mathcal{L}u_1 = -ie^{i[\theta+\Theta]}\boldsymbol{v}\cdot\nabla U.
$$

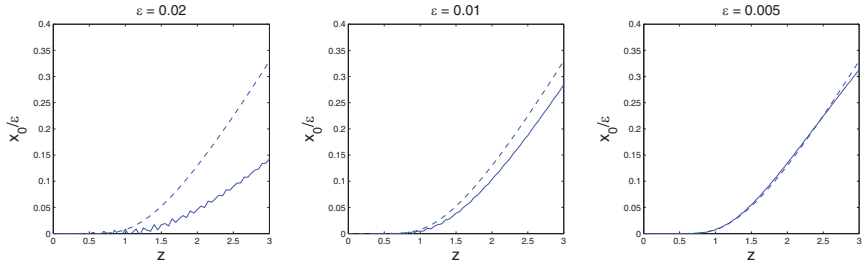

(a) $\epsilon = 0.02$ (b) $\epsilon = 0.01$ (c) $\epsilon = 0.005$

FIG. 7. *Difference between scaled solitary wave positions x_0 (solid) in the NLSE equation and free boundary problem (dashed) for various ϵ.*

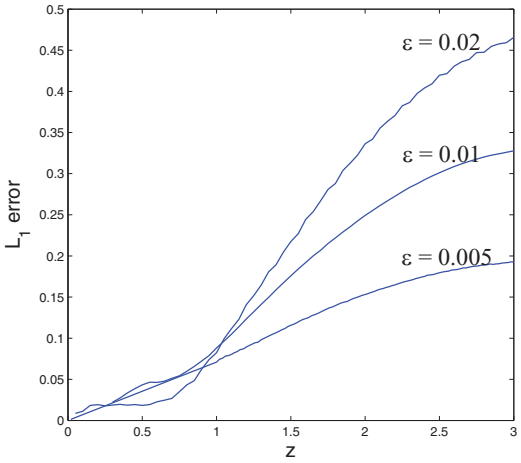

FIG. 8. *Difference between the outer solutions in the NLSE* (1) *and free boundary* (53) *models, measured as the L_1 distance on an interval excluding the solitary wave.*

The imaginary part of the $e^{i\theta}$ mode of this equation reads

$$-\lambda\eta + \Delta\eta + f(U^2)\eta = \boldsymbol{v}\cdot\nabla U, \tag{55}$$

which has a particular solution, $\frac{1}{2}(\boldsymbol{v}\cdot\boldsymbol{\xi})U$. The general solution which incorporates possible nullspace components is therefore

$$u_1 = e^{i\Theta}\Big\{A(z,Z)P_0 + A^*(z,Z)e^{2i\theta}Q_0 + i\big[\beta(z,Z) + \boldsymbol{v}\cdot\boldsymbol{\xi}/2\big]e^{i\theta}U + e^{i\theta}\boldsymbol{\mu}(z,Z)\cdot\nabla U\Big\}, \tag{56}$$

where, using the orthogonality relations (27), (28), one immediately has $\beta, \boldsymbol{\mu} = 0$. By matching, one has $e^{i\Theta}a(\lambda)A = \phi_0(x_0)$.

The next order equation ($O(\epsilon^1)$ terms in (17)) is $\mathcal{L}u_2 = e^{i\Theta}R_2$, where

$$\begin{aligned}-R_2 =& f'(U^2)U\Big([2A^2P_0Q_0 + A^2P_0^2]e^{-i\theta} + 2iA(\boldsymbol{v}\cdot\boldsymbol{\xi}/2)Q_0U\\ &+ [2|A|^2(P_0^2+Q_0^2+P_0Q_0) + (\boldsymbol{v}\cdot\boldsymbol{\xi}/2)^2U^2]e^{i\theta}\\ &+ 2iA^*(\boldsymbol{v}\cdot\boldsymbol{\xi}/2)P_0Ue^{2i\theta} + [2(A^*)^2Q_0P_0 + (A^*)^2Q_0^2]e^{3i\theta}\Big)\\ &+ \frac{1}{2}f''(U^2)U^3\Big(A^2(P_0+Q_0)^2e^{-i\theta} + 2|A|^2(P_0+Q_0)^2e^{i\theta}\\ &+ (A^*)^2(P_0+Q_0)^2e^{3i\theta}\Big) - i\boldsymbol{v}\cdot\nabla u_1 - U\Theta_z e^{i\theta}.\end{aligned} \tag{57}$$

The real part of the $e^{i\theta}$ component satisfies

$$\begin{aligned}-\lambda\eta+\Delta\eta+f(U^2)\eta+2f'(U^2)U^2\eta =& -f'(U^2)U\Big[2|A|^2(P_0^2+Q_0^2+P_0Q_0)+(\boldsymbol{v}\cdot\boldsymbol{\xi}/2)^2U^2\Big]\\ &- f''(U^2)U^3|A|^2(P_0+Q_0)^2 - \frac{1}{2}\boldsymbol{v}\cdot\nabla[(\boldsymbol{v}\cdot\boldsymbol{\xi})U] + \Theta_z U.\end{aligned} \tag{58}$$

There is a particular solution corresponding to the right-hand side terms $-f'(U^2)U^3(\boldsymbol{v}\cdot\boldsymbol{\xi}/2)^2 - \frac{1}{2}\boldsymbol{v}\cdot\nabla[(\boldsymbol{v}\cdot\boldsymbol{\xi})U] + \Theta_z U$, analogous to the one-dimensional solution (48),

$$u_{2part} = \Big[-\frac{1}{8}(\boldsymbol{v}\cdot\boldsymbol{\xi})^2U + (\Theta_z - |\boldsymbol{v}|^2/4)U_\lambda\Big]e^{i\theta}, \tag{59}$$

where again the orthogonality condition (26) recovers the slow phase Θ.

The Fourier decomposition of the equation for u_2 gives a coupled system for the $k = 0, 2$ modes

$$\Delta u_{20} + [f(U^2) + U^2f'(U^2)]u_{20} + U^2f'(U^2)u_{22}^* = R_{20}, \tag{60}$$

$$\Delta u_{22} - 2\lambda^2u_{22} + [f(U^2) + U^2f'(U^2)]u_{22} + U^2f'(U^2)u_{20}^* = R_{22}, \tag{61}$$

where $u_{2k} = \hat{u}_2(k,\cdot)$ and

$$-R_{20} = iA\Big\{2f'(U^2)U^2(\boldsymbol{v}\cdot\boldsymbol{\xi}/2)Q_0 - \boldsymbol{v}\cdot\nabla P_0\Big\}, \tag{62}$$

$$-R_{22} = iA^*\Big\{2f'(U^2)U^2(\boldsymbol{v}\cdot\boldsymbol{\xi}/2)P_0 - \boldsymbol{v}\cdot\nabla Q_0\Big\}. \tag{63}$$

A solvability condition for (60)–(61) results from taking an inner product with the real and imaginary parts using the nullspace vectors $[P_0, Q_0]$ and $[P_0, -Q_0]$, respectively. The result (after using the Green's identity for the left-hand side) gives zero simply by virtue of symmetry,

$$\lim_{r\to\infty}\int_{|\boldsymbol{\xi}|=r}\nabla u_{20}\cdot\boldsymbol{n}d\boldsymbol{\xi} = 0. \tag{64}$$

Note that this precludes the logarithmic behavior $u_{20} \sim C\ln|\boldsymbol{\xi}|$ for $|\boldsymbol{\xi}| \to \infty$. The complete solution for u_2 also includes the nullspace components $\cos(m\varphi)[P_1(r) + e^{2i\theta}Q_1(r)]$ and $\sin(m\varphi)[P_1(r) + e^{2i\theta}Q_1(r)]$. These simply accommodate matching to the gradient of the outer solution at leading order

$$\lim_{\boldsymbol{\xi}\to\infty}\nabla u_2 = \nabla\psi(\boldsymbol{x}_0, z), \tag{65}$$

which means, in particular, that ϕ_0 is continuously differentiable at x_0.

Finally, the equation for the $k = 0$ mode of the third order expansion equation u_{30} will be required later. It satisfies an equation of the form

$$\begin{aligned}\Delta u_{30} = &- f'(U^2)|A|^2 A P_0^3 - iA_z P_0 + i\boldsymbol{v}\cdot\nabla u_2 \\ &+ \text{ terms which decay exponentially as } |\boldsymbol{\xi}| \to 0\ .\end{aligned} \tag{66}$$

Only the terms which do not decay exponentially will be needed to determine the far-field behavior which appears in the leading order expression for momentum flux.

4.2. Expansion for $m(\lambda) \neq 0$. The possibility of logarithmic behavior for $\boldsymbol{\xi} \to \infty$ resulting from the eigenfunction component P_0 would suggest an expansion in powers of $1/|\ln\epsilon|$. This not a practical approach, however, since many terms in such an expansion would be required for a suitably accurate approximation. A better alternative, formulated by Ward, Henshaw, and Keller [50], implicitly sums the logarithmic contributions in such an expansion. The outer solution is expanded,

$$\psi = \psi_0(\boldsymbol{\xi}, z; \chi(\epsilon)) + \chi(\epsilon)\psi_1 + \cdots,$$

where ψ_0 has a logarithmic singularity at $\boldsymbol{x}_0$. The asymptotics of the singularity and the order function $\chi(\epsilon)$ will be uniquely determined by matching.

The expansion term u_1 satisfies the same equation as before, and the most general solution is given by (56). On the other hand, one has $u_1 \sim e^{i\Theta} A m(\lambda)\ln|\xi|$ for large $|\xi|$, which would require an $O(|\ln\epsilon|)$ term in the outer solution. Since this possibility has been eliminated by the hypothesis that the outer solution has $O(1)$ amplitude, it follows that $A = 0$.

The logarithmic order term $u_\dagger$ satisfies $\mathcal{L}u_\dagger = 0$, and so the solution will be (after applying orthogonality conditions)

$$u_\dagger = e^{i\Theta}\Big\{A_\dagger P_0 + A_\dagger^* e^{2i\theta} Q_0\Big\}. \tag{67}$$

Since, as $|\boldsymbol{\xi}| \to \infty$,

$$u \sim \chi(\epsilon) e^{i\Theta} A_\dagger [m(\lambda)\ln|\boldsymbol{\xi}| + a(\lambda)] + o(1),$$

matching requires

$$\psi_0 \sim \chi(\epsilon) e^{i\Theta} A_\dagger \left(m(\lambda)\ln\left|\frac{\boldsymbol{x}-\boldsymbol{x}_0}{\epsilon}\right| + a(\lambda)\right) + o(1), \quad \boldsymbol{x} \to \boldsymbol{x}_0. \tag{68}$$

With the choice

$$\chi(\epsilon) = \frac{1}{-m(\lambda)\ln\epsilon + a(\lambda)},$$

relation (68) gives the required singularity condition

$$\psi_0 \sim e^{i\Theta} A_\dagger + e^{i\Theta} A_\dagger m(\lambda)\chi(\epsilon)\log|\boldsymbol{x}-\boldsymbol{x}_0| + o(1), \quad \boldsymbol{x} \to \boldsymbol{x}_0. \tag{69}$$

Given any outer solution ψ_0 with a logarithmic singularity at $\boldsymbol{x}_0$, it can be decomposed as

$$\psi_0 = \psi_R + 2\pi e^{i\Theta} A_\dagger m(\lambda)\chi(\epsilon) G(x; x_0), \quad \psi_R \text{ bounded at } \boldsymbol{x}_0, \tag{70}$$

where

$$G \sim \frac{1}{2\pi} \ln |\boldsymbol{x} - \boldsymbol{x}_0| + O(|\boldsymbol{x} - \boldsymbol{x}_0|^2), \quad \boldsymbol{x} \to \boldsymbol{x}_0. \tag{71}$$

Construction of such a G is explained below in the context of numerical implementation. It follows from (69) that

$$\psi_R(x_0) = e^{i\Theta} A_\dagger, \tag{72}$$

which determines the singularity constant $A_\dagger$.

For the expansion term u_2, the right-hand side of the corresponding linear equation is $e^{i\Theta} R_2$, where

$$-R_2 = f'(U^2) U^3 (\boldsymbol{v} \cdot \boldsymbol{\xi}/2)^2 e^{i\theta} - i\boldsymbol{v} \cdot \nabla u_1 - U\Theta_z e^{i\theta}, \tag{73}$$

which has the same particular solution given previously in (59). The complete solution for u_2 has nullspace components $\cos(m\varphi)[P_1(r) + e^{2i\theta} Q_1(r)]$ and $\sin(m\varphi)[P_1(r) + e^{2i\theta} Q_1(r)]$, which grow linearly as $\boldsymbol{\xi} \to \infty$. In this case, matching to the outer solution is facilitated by the decomposition (70), which gives

$$\lim_{\boldsymbol{\xi} \to \infty} \nabla u_2(\boldsymbol{\xi}) = \nabla \psi_R(x_0). \tag{74}$$

For $u_{\dagger\dagger}$ and $u_{\dagger\dagger\dagger}$ the corresponding right-hand sides $R_{\dagger\dagger}$ and $R_{\dagger\dagger\dagger}$ split the nonlinear contributions in (57):

(75)

$$-R_{\dagger\dagger} = f'(U^2) U \Big(2iA_\dagger (\boldsymbol{v} \cdot \boldsymbol{\xi}/2) Q_0 U + 2iA_\dagger^* (\boldsymbol{v} \cdot \boldsymbol{\xi}/2) P_0 U e^{2i\theta} \Big),$$

(76)

$$\begin{aligned} -R_{\dagger\dagger\dagger} = {} & f'(U^2) U \Big([2A_\dagger^2 P_0 Q_0 + A_\dagger^2 P_0^2] e^{-i\theta} + 2|A_\dagger|^2 (P_0^2 + Q_0^2 + P_0 Q_0) e^{i\theta} \\ & + [2(A_\dagger^*)^2 Q_0 P_0 + (A_\dagger^*)^2 Q_0^2] e^{3i\theta} \Big) \\ & + \frac{1}{2} f''(U^2) U^3 \Big(A_\dagger^2 (P_0 + Q_0)^2 e^{-i\theta} + 2|A_\dagger|^2 (P_0 + Q_0)^2 e^{i\theta} + (A_\dagger^*)^2 (P_0 + Q_0)^2 e^{3i\theta} \Big). \end{aligned}$$

These lead to a systems similar to (60)–(61) for the $k = 0, 2$ Fourier modes, labeled $u_{\dagger\dagger 0,2}$ and $u_{\dagger\dagger\dagger 0,2}$. The corresponding solvability argument is somewhat different. Suppose that the far-field behavior of $u_{\dagger\dagger 0}$ is

$$u_{\dagger\dagger 0} \sim C_1 \ln |\boldsymbol{\xi}| + C_2, \quad |\xi| \to \infty. \tag{77}$$

As before, we multiply the real and imaginary parts of the linear system for $u_{\dagger\dagger 0,2}$ by the nullspace vectors $[P_0, Q_0]$ and $[P_0, -Q_0]$, respectively. Integrating both sides on a disk of radius r gives (after using the Green's identity)

$$\int_{|\boldsymbol{\xi}|=r} P_0 \nabla u_{\dagger\dagger 0} \cdot \boldsymbol{n} - u_{\dagger\dagger 0} \nabla P_0 \cdot \boldsymbol{n} \, d\boldsymbol{\xi} \sim 0, \quad r \to \infty. \tag{78}$$

By virtue of (77) this implies $a(\lambda) C_1 - m(\lambda) C_2 = 0$, with a similar result holding for $u_{\dagger\dagger\dagger}$. It follows that there exist constants $A_{\dagger\dagger}, A_{\dagger\dagger\dagger}$ so that

$$u_{\dagger\dagger} \sim e^{i\Theta} A_{\dagger\dagger} (m(\lambda) \ln |\boldsymbol{\xi}| + a(\lambda)), \tag{79}$$

$$u_{\dagger\dagger\dagger} \sim e^{i\Theta} A_{\dagger\dagger\dagger} (m(\lambda) \ln |\boldsymbol{\xi}| + a(\lambda)), \tag{80}$$

as $\boldsymbol{\xi} \to \infty$. In the next section, these results are used to identify the flux of solitary wave power.

4.3. Modulation of solitary wave parameters. To leading order, the power of the inner solution on the left-hand side of (22) is

$$\int_{|\boldsymbol{\xi}|<r} |u|^2 d\boldsymbol{\xi} \sim \epsilon^{-2} \int U(|\boldsymbol{\xi}|,\lambda)^2 \, d\boldsymbol{\xi} = \epsilon^{-2} I_0(\lambda), \quad \epsilon \to 0, r \to \infty. \tag{81}$$

Since u_0 has radial symmetry, using (56), the leading order momentum on the left-hand side of (23) is

$$\begin{aligned} \int_{|\boldsymbol{\xi}|<r} 2\mathrm{Im}[u^* \nabla u] d\boldsymbol{\xi} &\sim 2\epsilon^{-1} \mathrm{Im} \int u_0^* \nabla u_1 + u_1^* \nabla u_0 \, d\boldsymbol{\xi} \\ &= \epsilon^{-1} \boldsymbol{v} \int U(|\boldsymbol{\xi}|,\lambda)^2 \, d\boldsymbol{\xi} = \epsilon^{-1} \boldsymbol{\Pi}_0(\lambda, \boldsymbol{v}), \quad \epsilon \to 0, r \to \infty. \end{aligned} \tag{82}$$

The case $m(\lambda) = 0$ and corresponding expansion are discussed first. To begin with, we illustrate the roles of the expansion terms by considering a more general situation,

$$u_2 \sim e^{i\Theta} \{A_2 + \boldsymbol{B} \cdot \boldsymbol{\xi} + M \ln |\boldsymbol{\xi}|\} + O(|\boldsymbol{\xi}|^{-1}), \quad |\boldsymbol{\xi}| \to \infty. \tag{83}$$

With the choice of slow scale $Z = \epsilon z$, the modulation of the power (22) is therefore asymptotically

$$\frac{dI_0(\lambda)}{dZ} \sim 2\mathrm{Im} \left\{ \lim_{r\to\infty} \int_{|\boldsymbol{\xi}|=r} u_1(r\boldsymbol{\xi}, \cdot) \nabla u_2^* \cdot \boldsymbol{n} \, d\boldsymbol{\xi} \right\} = 4\pi \mathrm{Im}(AM^*), \quad \epsilon \to 0. \tag{84}$$

In terms of the expansion, the momentum flux in the scaled moving frame (21) is asymptotically

$$\begin{aligned} \boldsymbol{T}_m \sim &- \Big\{ 2|\nabla u_2|^2 + u_1 \Delta u_3^* + u_1^* \Delta u_3 + G(|u_1|^2) \Big\} \mathbf{Id} \\ &+ 4\mathrm{Re}(\nabla u_2 \otimes \nabla u_2^*) - 2\mathrm{Im}[u_1^* \nabla u_2] \otimes \boldsymbol{v} + O(\epsilon), \quad \epsilon \to 0, |\boldsymbol{\xi}| \to \infty. \end{aligned} \tag{85}$$

Using (83) and the far-field behavior (66), the double limit $\epsilon \to 0, |\boldsymbol{\xi}| \to \infty$ yields

$$\begin{aligned} \boldsymbol{T}_m \sim &- \Big\{ [2(\boldsymbol{B}M^* + \boldsymbol{B}^* M) + i(A^* M - AM^*)\boldsymbol{v}] \cdot \boldsymbol{\xi}/|\boldsymbol{\xi}|^2 \Big\} \mathbf{Id} \\ &+ 4\mathrm{Re}\Big(M^* \boldsymbol{B} \otimes (\boldsymbol{\xi}/|\boldsymbol{\xi}|^2) + M(\boldsymbol{\xi}/|\boldsymbol{\xi}|^2) \otimes \boldsymbol{B}^* \Big) \\ &- 2\mathrm{Im}[A^* M \boldsymbol{\xi}/|\boldsymbol{\xi}|^2] \otimes \boldsymbol{v} + C\mathbf{Id} + O(|\boldsymbol{\xi}|^{-2}), \end{aligned} \tag{86}$$

where $C\mathbf{Id}$ represents the $\boldsymbol{\xi}$-independent isotropic part whose flux integral is zero. The momentum flux (23) then evaluates to

$$\frac{d\boldsymbol{\Pi}_0(\lambda, \boldsymbol{v})}{dZ} \sim -8\pi \mathrm{Re}(M^* \boldsymbol{B}), \quad \epsilon \to 0. \tag{87}$$

The results (84) and (87) can be checked using Galilean symmetry; see Appendix B.

In the case of $m(\lambda) = 0$, (64) gives $M = 0$ in (83). This means that the leading order power and momentum fluxes are zero, at least on the timescale $Z = \epsilon z$. Although it may happen that matching to correction terms in the outer solution might yield modulation on an even slower scale, this possibility is not pursued here.

For the case where $m(\lambda) \neq 0$, the situation is qualitatively different. The power flux (20) is to leading order

(88)
$$\boldsymbol{j}_m \sim 2\mathrm{Im}\left[\chi(\epsilon)^2(u_\dagger \nabla u^*_{\dagger\dagger} + u_{\dagger\dagger}\nabla u^*_\dagger) + \chi(\epsilon)^3(u_\dagger \nabla u^*_{\dagger\dagger\dagger} + u_{\dagger\dagger\dagger}\nabla u^*_\dagger)\right], \quad \epsilon \to 0, |\boldsymbol{\xi}| \to \infty.$$

For large $|\boldsymbol{\xi}|$, applying (79) and (80) shows that the term in brackets is strictly real. It follows that solitary wave power is modulated, at most, on a slow timescale $Z = \epsilon z$. On the other hand, the leading order momentum flux (21) is

(89)
$$\boldsymbol{T}_m \sim -\frac{\chi(\epsilon)}{\epsilon}\Big\{2(\nabla u_\dagger \cdot \nabla u^*_2 + \nabla u^*_\dagger \cdot \nabla u_2)\mathbf{Id} + 4\mathrm{Re}(\nabla u_\dagger \otimes \nabla u^*_2 + \nabla u_2 \otimes \nabla u^*_\dagger)\Big\}, \ \epsilon \to 0, |\boldsymbol{\xi}| \to \infty.$$

With $u_\dagger \sim M \ln|\xi|$ and $\nabla u_2 \sim \boldsymbol{B}$ as $\xi \to \infty$, this becomes

(90)
$$\boldsymbol{T} \sim -2[\boldsymbol{B}M^* + \boldsymbol{B}^* M]\mathbf{Id} + 4\mathrm{Re}\Big(M^*\boldsymbol{B}(\boldsymbol{\xi}/|\boldsymbol{\xi}|^2) + M(\boldsymbol{\xi}/|\boldsymbol{\xi}|^2)\otimes \boldsymbol{B}^*\Big), \quad \epsilon \to 0, |\boldsymbol{\xi}| \to \infty.$$

The matching conditions (72) and (74) imply that $\boldsymbol{B} = \nabla\psi_R(x_0)$ and $M = \psi_R(x_0)$, and therefore with the choice $Z = \chi(\epsilon)$, momentum balance in (23) yields

$$\frac{d\boldsymbol{\Pi}_0(\lambda, \boldsymbol{v})}{dZ} \sim -8\pi\mathrm{Re}\Big[\psi^*_R(x_0)\nabla\psi_R(x_0)\Big]. \tag{91}$$

4.4. Free singularity problem. For the $m \neq 0$ case, the preceding two sections indicate that the dynamics can be described by a reduced problem which couples a singular outer solution to the position of the solitary wave. This problem can be summarized as a "free singularity problem" for unknowns $\psi, A, \boldsymbol{x}_0$:

$$i\psi_z + \Delta\psi + |\psi|^2\psi = 0, \quad \boldsymbol{x} \neq \boldsymbol{x}_0, \tag{92}$$

(93)
$$\psi \sim A(z) + A(z)m(\lambda)\chi(\epsilon)\ln|\boldsymbol{x} - \boldsymbol{x}_0(z)| + o(1), \quad \boldsymbol{x} \to \boldsymbol{x}_0,$$

(94)
$$\boldsymbol{x}_0''(z) = -\frac{8\pi\chi(\epsilon)}{I_0(\lambda)}\mathrm{Re}\Big[\psi^*_R(\boldsymbol{x}_0)\nabla\psi_R(\boldsymbol{x}_0)\Big], \quad \psi_R(\boldsymbol{x}_0) = \psi - A(z)m(\lambda)\chi(\epsilon)G(\boldsymbol{x}, \boldsymbol{x}_0(z)),$$

where the subscripts have been dropped and the phase factor has been absorbed into A. Logically this is to be solved with an initial condition $\psi(\boldsymbol{x}, 0)$ which obeys the singularity condition, along with position and velocity initial data $\boldsymbol{x}_0(0)$ and $\boldsymbol{x}_0'(0)$. We are not aware of any existence results for problems of this type. On the other hand, there does seem to be a reliable numerical implementation, which is described next.

4.5. Numerical verification. Two-dimensional computations of the original equation (1) with the cubic-quintic nonlinearity (8) have been conducted. The same numerical methods used for the one-dimensional problem and outlined in Appendix A were implemented for (92). All computations were performed on a square domain $[-L/2, L/2]^2$, where $L = 20$, endowed with periodic boundary conditions.

The initial condition used in all the tests below is an exact solitary wave, combined with a traveling, dispersing Gaussian wavepacket

$$\psi(\boldsymbol{x}, 0) = \epsilon^{-1}U\left(\frac{\boldsymbol{x} - \boldsymbol{x}_0}{\epsilon}; \lambda\right) + w(\boldsymbol{x}), \quad w(\boldsymbol{x}) = E\exp(i\boldsymbol{v}_a\boldsymbol{x} + |\boldsymbol{x} - \boldsymbol{x}_a|^2/W). \tag{95}$$

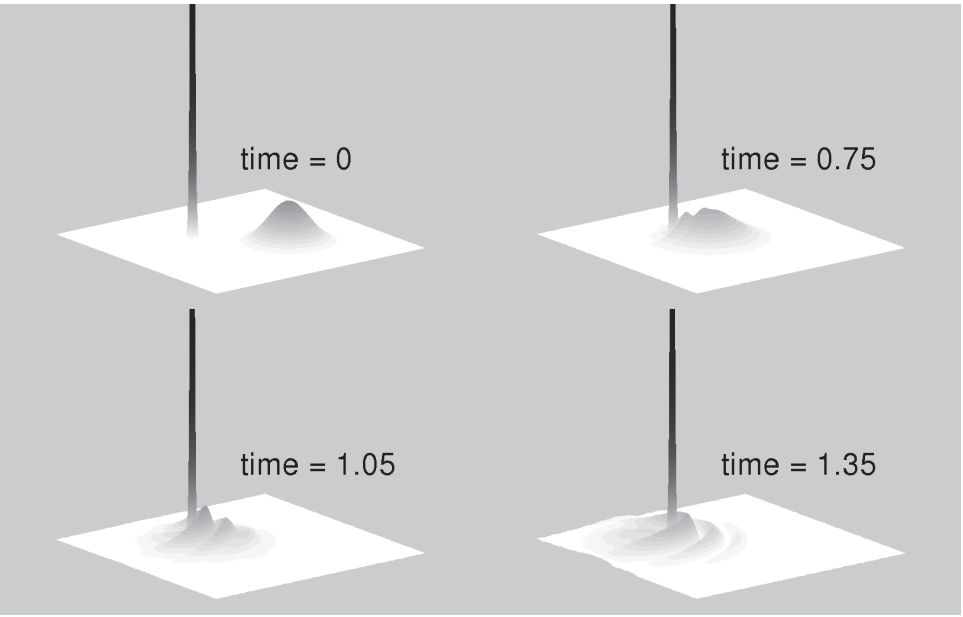

FIG. 9. *Evolution of* (1) *for* $\lambda = 0.04$ *where* $m \neq 0$. *Shown is a shaded three-dimensional plot of the modulus* $|\psi|$. *The initial conditions were chosen so that the Gaussian wavepacket on the right will move toward the solitary wave on the left. Momentum is transferred between the two waves.*

The fixed parameters were $\boldsymbol{x}_0 = (-2, 2)$, $\boldsymbol{x}_a = (2, -2)$, $\boldsymbol{v}_a = (-2, 2)$, $E = 0.5$, and $W = 3$.

We first illustrate the difference between the logarithmic and nonlogarithmic cases. The parameters were $\epsilon = 0.025$, and both $\lambda = 0.04$ and $\lambda = 0.077$ were tried. The former gives a ratio $m(\lambda)/a(\lambda)$ equal to -0.25, whereas the latter gives a ratio which is roughly zero. Figures 9 and 10 show the evolution of (1) for the two different cases. The qualitative predictions of the analysis are born out: there is strong interaction when $m(\lambda)$ is far from zero, and essentially no interaction when $m(\lambda) \approx 0$. In the former case, some momentum is imparted to the solitary wave in the direction of motion of the wavepacket.

A quantitative comparison between the full equation (1) and the free singularity problem (92) was also conducted. Here $\lambda = 0.04$ is fixed and ϵ was varied, using the same initial condition (95) as before. For the free singularity problem, the initial condition was just the Gaussian wave $\psi(\boldsymbol{x}, 0) = w(\boldsymbol{x})$.

Although the decomposition (70) could employ any smooth function G with the correct asymptotic behavior, we have found good performance using the Laplacian modified Green's function. This function $G(\boldsymbol{x}, \boldsymbol{x}_0) = G_0(\boldsymbol{x} - \boldsymbol{x}_0)$ is obtained from solving the problem

$$\Delta G_0 = \delta(\boldsymbol{x}) - \frac{1}{L^2}, \quad G_0(0) = 0, \quad G_0(\boldsymbol{x}) = G_0(\boldsymbol{x} + \boldsymbol{p}), \quad \boldsymbol{p} \in L\mathbb{Z}^2.$$

In practice, this is obtained numerically by a decomposition into a singular and a regular part,

$$\Delta G_R = -\Delta S - \frac{1}{L^2}, \quad S \equiv \frac{1}{4\pi} \ln |\sin^2(x) + \sin^2(y)|,$$

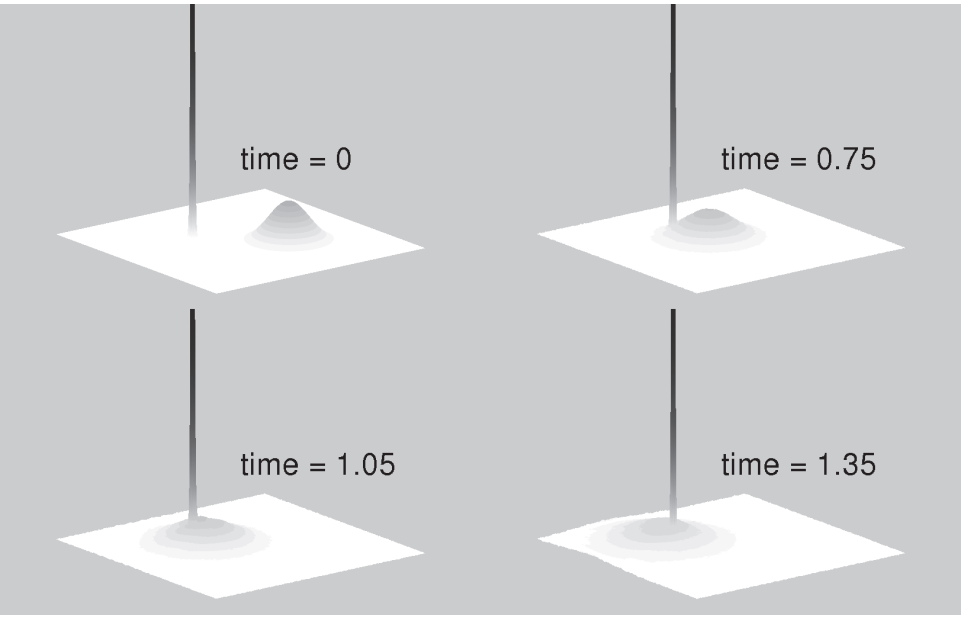

FIG. 10. *Evolution of* (1) *for* $\lambda = 0.077$ *where* $m \approx 0$. *In this case, there is no conspicuous interaction between the two waves.*

where the first equation is subject to periodic boundary conditions. The regular part G_R is easily found in the context of a Fourier pseudospectral discretization, and suitably shifted so that $G_R(0) = 0$. Then $G(\boldsymbol{x}, \boldsymbol{x}_0)$ is computed by table lookup for $G_R(\boldsymbol{x} - \boldsymbol{x}_0)$ combined with the exact expression for S.

We now turn to how the singularity constant A is computed. Given $\boldsymbol{x}_0(z)$ at some step z, the four grid points nearest to x_0 can be used to produce a bilinear interpolation of $\psi - A(z)m(\lambda)\chi(\epsilon)G(\boldsymbol{x}, \boldsymbol{x}_0(z))$ called $\psi_{RB}(\boldsymbol{x}, z; A) \approx \psi_R$. Using (93), the unknown coefficient A then solves the linear problem

$$A = \psi_{RB}(\boldsymbol{x}_0, z; A).$$

Determining A allows construction of the regular part ψ_R of the solution, which is needed to evaluate the acceleration term (94).

Solutions of (1) at values $\epsilon = 0.025, 0.0125, 0.00625$ were compared to the numerical solution of (92)–(94). As in the one-dimensional case, the displacement of the solitary wave was computed as a function of z during the collision period, clearly indicating a transfer of momentum (Figure 11).

We have also computed the difference between the singular solution ψ_S solving (92)–(94) and the solution of the original NLSE (1) for various ϵ. This difference was defined similarly to the one-dimensional case as

$$L_1 \text{ Error} = \int_D |\psi_S - \psi| \, dx,$$

where $D = \{\boldsymbol{x} \in [-L/2, L/2]^2, |\boldsymbol{x} - \boldsymbol{x}_0| > 15\epsilon\}$. Figure 12 shows the evolution of this quantity for various ϵ. The agreement between the two models improves with decreasing ϵ.

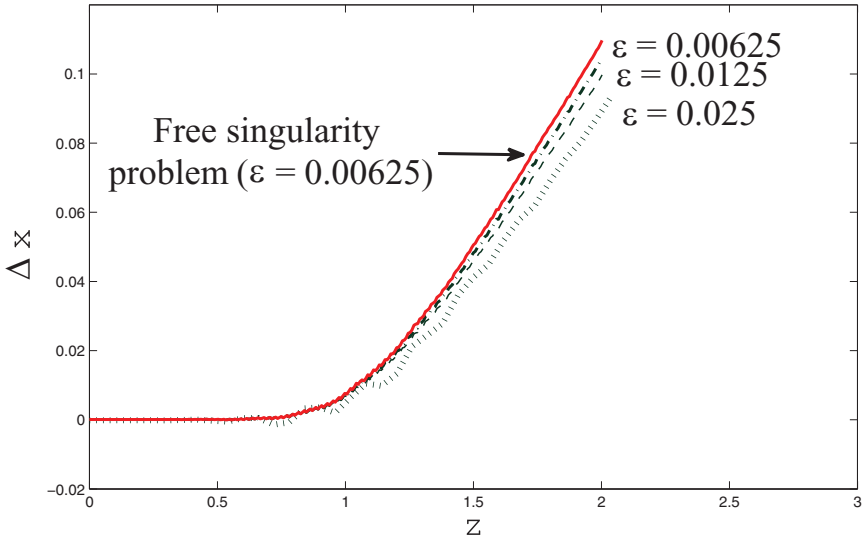

FIG. 11. *A comparison of the solitary wave displacement* Δx *in* (1) *for* $\epsilon = 0.025$ *(dotted),* $\epsilon = 0.0125$ *(dashed),* $\epsilon = 0.00625$ *(dot-dashed), along with the displacement predicted by a numerical solution to* (92)–(94) *(solid).*

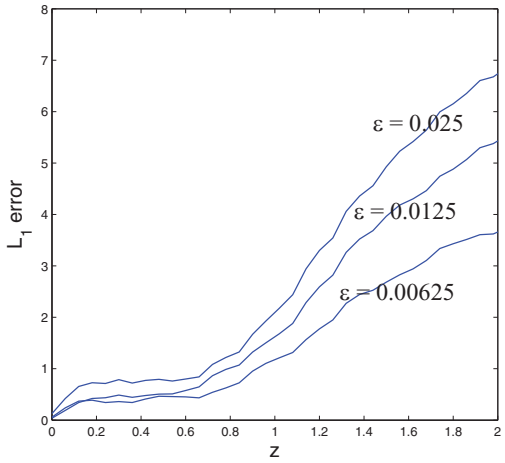

FIG. 12. *Difference between the outer solutions in the NLSE* (1) *and free singularity problems* (92)–(94) *measured as the* L_1 *norm of the difference on a subdomain excluding the solitary wave.*

5. Conclusion. This paper considers a singular perturbation of the cubic nonlinear Schrödinger equation. In two dimensions, this perturbation has the effect of alleviating the well-known self-focusing singularity. Small saturation leads to solitary wave solutions with fine-scale behavior in all dependent variables. Such a situation poses enormous difficulty for numerical simulation. The asymptotic analysis presented herein removes the fine scales completely, leading to free boundary (in one dimension) and free singularity (in two dimensions) problems which are considerably more numerically tractable. These can be viewed as a type of nonlinear stability result for

solitary waves since the perturbations evolve under a genuinely nonlinear equation (see (92)).

We have excluded a variety of phenomena in this study. In problems involving optical propagation, time dependence may arise from group velocity dispersion. Depending on the sign of the dispersion, this effect may arrest the self-focusing singularity [32]. Another excluded effect is the possibility of internal modes [38], which are long-lived transient oscillations of solitary waves. These were never observed in our simulations, perhaps because they exist over a limited range of parameters.

Our methodology is likely extensible for a variety of problems which involve localized coherent structures interacting with a slowly varying environment. We have obtained results similar to those presented here for a modified NLSE which includes a delayed nonlinear response associated with Raman scattering [19]. In this case, the delay term gives nontrivial modulation of solitary wave power, which was not observed here.

Partial differential equations with dynamic free singularities like the one derived appear to be an entirely new class of free boundary evolution. We are not aware of any specific rigorous or heuristic analysis of such problems. A more thorough understanding of this class of equations is a challenge for future research.

Appendix A. Conservative numerical scheme. The numerical method used to compute (1) is adapted from the power-conserving scheme detailed in [41]. We have made a few modifications to this idea which appear to improve the overall performance.

Suppose that the timestep h and two sequential steps ψ_{n-1} and ψ_n are provided, where $\psi_n \approx \psi(nh)$. Let $\psi_e = \psi_n + \frac{1}{2}(\psi_n - \psi_{n-1})$ be the extrapolation of the solution at $z = (n + \frac{1}{2})h$. Suppose that k is a complex-valued parameter to be determined, with $k \approx 1$ and $|k| = 1$. Let ψ_p be an approximation of the solution at $z = (n + \frac{1}{2})h$ obtained from the semi-implicit timestepping method

$$\left(I - \frac{1}{2}ih\Delta\right)\psi_p = \psi_n + \frac{ikh}{2}F(|\psi_e|^2)|\psi_e|. \tag{96}$$

A pseudospectral discretization in space is employed, making the operator on the left easy to invert by a fast Fourier transform. Provided $k = 1 + O(h)$, this method is formally first order accurate. The approximate solution at $z = (n+1)h$ is then obtained from a further linear extrapolation $\psi_{n+1} = 2\psi_p - \psi_n$. It is useful to decompose the solution to (96) as $\psi_p = \psi_0 + k\psi_1$, where

$$\left(I - \frac{1}{2}ih\Delta\right)\psi_0 = \psi_n, \tag{97}$$

$$\left(I - \frac{1}{2}ih\Delta\right)\psi_1 = \frac{ih}{2}F(|\psi_e|^2)|\psi_e|. \tag{98}$$

We now want to choose k so that power is conserved. Letting D be the spatial domain,

$$\int_D |\psi_{n+1}|^2 - |\psi_n|^2\,dx = 2\int_D (\psi_p - \psi_n)\psi_p^* + (\psi_p - \psi_n)^*\psi_p\,dx \tag{99}$$

$$= ih\int_D [\psi_p^*\Delta\psi_p - \psi_p\Delta\psi_p^*] + F(|\psi_e|^2)(\psi_e\psi_p^* - \psi_e^*\psi_p)\,dx = 0, \tag{100}$$

provided, using (97)–(98),

(101)
$$0 = \int_D F(|\psi_e|^2)(\psi_e\psi_p^* - \psi_e^*\psi_p)\,dx = \int_D F(|\psi_e|^2)[k\psi_e(\psi_0+k\psi_1)^* - k^*\psi_e^*(\psi_0+k\psi_1)]\,dx.$$

The bracketed term in (100) vanishes when the Green's identity is employed, under either periodic or Neumann boundary conditions. It can be shown that a spatially discretized version of (99)–(100) also holds.

With the property that k has unit modulus, (101) can be written as

(102)
$$I + kJ - k^*J = 0, \quad I = \int_D F(|\psi_e|^2)(\psi_e\psi_1^* - \psi_e^*\psi_1)\,dx, \quad J = \int_D F(|\psi_e|^2)\psi_e\psi_0^*\,dx.$$

Note that I is pure imaginary, whereas k and J can be put into polar form,

$$k = \exp(i\phi_k), \quad J = \exp(i\phi_J)|J|,$$

which, plugging into (102), leads to

$$\phi_K = \sin^{-1}\left(\frac{iI}{2|J|}\right) - \phi_J.$$

Note that I is formally of size $O(h)$, and since $\psi_e - \psi_0 = O(h)$, it follows that ϕ_J is also $O(h)$. Altogether, this means that $\phi_k = O(h)$ and $k = 1 + O(h)$, as required.

Appendix B. Galilean symmetry of modulation equations. Here we verify that the modulation equations (84) and (87) respect the underlying Galilean symmetry of (1). Let $\boldsymbol{v}_0$ be the velocity of any moving reference frame. The corresponding transformation of quantities $A, M, \boldsymbol{B}$ is

(103)
$$\begin{aligned} &A' = \exp(i\boldsymbol{v}_0[\boldsymbol{x}_0/2 - z/4])A, \quad M' = \exp(i\boldsymbol{v}_0[\boldsymbol{x}_0/2 - z/4])M, \\ &\boldsymbol{B}' = \lim_{\boldsymbol{x}\to\boldsymbol{x}_0} \nabla\psi_0' = \exp(i\boldsymbol{v}_0[\boldsymbol{x}_0/2 - z/4])(i\boldsymbol{v}_0/2A + \boldsymbol{B}). \end{aligned}$$

The leading order solitary wave power and momentum in the moving frame are $I_0' = I_0$ and $\boldsymbol{\Pi}_0' = \boldsymbol{\Pi}_0 + \boldsymbol{v}_0 I_0$. On one hand, the modulation of momentum $\boldsymbol{\Pi}_0'$ can be computed using the untransformed relations (84) and (87), leading to

(104)
$$\frac{d\boldsymbol{\Pi}_0'}{dZ} = \frac{d\boldsymbol{\Pi}_0}{dZ} + \boldsymbol{v}_0\frac{dI_0}{dZ} = \Big[- 8\pi\mathrm{Re}(M^*\boldsymbol{B}) + 4\pi\boldsymbol{v}_0\mathrm{Im}(AM^*)\Big].$$

On the other hand, using the transformed version of (84) and (103) leads to

(105)
$$\frac{d\boldsymbol{\Pi}_0'}{dZ} = -8\pi\mathrm{Re}(M'^*\boldsymbol{B}') = -8\pi\mathrm{Re}(M^*[i\boldsymbol{v}_0A/2 + \boldsymbol{B}]) = \Big[-8\pi\mathrm{Re}(M^*\boldsymbol{B}) + 4\pi\boldsymbol{v}_0\mathrm{Im}(AM^*)\Big],$$

which is the same as (104).

REFERENCES

[1] G. Assanto and M. A. Karpierz, *Nematicons: Self-localised beams in nematic liquid crystals*, Liquid Crystals, 36 (2009), pp. 1161–1172.

[2] P. Béjot, J. Kasparian, S. Henin, V. Loriot, T. Vieillard, E. Hertz, O. Faucher, B. Lavorel, and, J.-P. Wolf, *Higher-Order Kerr Terms Allow Ionization-Free Filamentation in Gases*, preprint, arXiv:1011.1598, 2010.

[3] L. Berge, *Wave collapse in physics: Principles and applications to light and plasma waves*, Phys. Rep., 303 (1998), pp. 259–370.
[4] L. Bergé and A. Couairon, *Gas-induced solitons*, Phys. Rev. Lett., 86 (2001), pp. 1003–1006.
[5] L. Bergé, C. Gouédard, J. Schjodt-Eriksen, and H. Ward, *Filamentation patterns in Kerr media vs. beam shape robustness, nonlinear saturation and polarization states*, Phys. D, 176 (2003), pp. 181–211.
[6] L. Bergé, M. R. Schmidt, J. J. Rasmussen, P. L. Christiansen, and K. Ø. Rasmussen, *Amalgamation of interacting light beamlets in Kerr-type media*, J. Opt. Soc. Amer. B Opt. Phys., 14 (1997), pp. 2550–2562.
[7] L. Bergé, S. Skupin, R. Nuter, J. Kasparian, and J.-P. Wolf, *Ultrashort filaments of light in weakly ionized, optically transparent media*, Rep. Progr. Phys., 70 (2007), pp. 1633–1713.
[8] A. Biswas, *Perturbation of solitons with non-Kerr law nonlinearity*, Chaos Solitons Fractals, 13 (2002), pp. 815–823.
[9] M. Centurion, Y. Pu, M. Tsang, and D. Psaltis, *Dynamics of filament formation in a Kerr medium*, Phys. Rev. A, 71 (2005), 063811.
[10] P. Chernev and V. Petrov, *Self-focusing of light pulses in the presence of normal group-velocity dispersion*, Optics Lett., 17 (1992), pp. 172–174.
[11] C. Elphick, E. Meron, and E. A. Spiegel, *Patterns of propagating pulses*, SIAM J. Appl. Math., 50 (1990), pp. 490–503.
[12] G. Fibich, *Some modern aspects of self-focusing theory*, in Self-Focusing: Past and Present, Springer, New York, 2009, pp. 413–438.
[13] G. Fibich, S. Eisenmann, B. Ilan, and A. Zigler, *Control of multiple filamentation in air*, Optics Lett., 29 (2004), pp. 1772–1774.
[14] G. Fibich, N. Gavish, and X. Wang, *New singular solutions of the nonlinear Schrödinger equation*, Phys. D, 211 (2005), pp. 193–220.
[15] G. Fibich and M. Klein, *Continuations of the nonlinear Schrödinger equation beyond the singularity*, Nonlinearity, 24 (2011), pp. 519–552.
[16] G. Fraiman, *The asymptotic stability of the manifold of self-similar solutions in the presence of self-focusing*, Zh. Eksp. Teor. Fiz., 88 (1985), pp. 390–400.
[17] V. Gerdjikov, D. Kaup, I. Uzunov, and E. Evstatiev, *Asymptotic behavior of n-soliton trains of the nonlinear Schrödinger equation*, Phys. Rev. Lett., 77 (1996), pp. 3943–3946.
[18] J. Ginibre and G. Velo, *On a class of nonlinear Schrödinger equations.* I. *The Cauchy problem, general case*, J. Funct. Anal., 32 (1979), pp. 1–32.
[19] K. B. Glasner and J. Allen-Flowers, *The effect of Raman scattering on optical filaments*, in preparation, 2015.
[20] K. Gorshkov and L. Ostrovsky, *Interactions of solitons in nonintegrable systems: Direct perturbation method and applications*, Phys. D, 3 (1981), pp. 428–438.
[21] M. Grillakis, *Linearized instability for nonlinear Schrödinger and Klein-Gordon equations*, Comm. Pure Appl. Math., 41 (1988), pp. 747–774.
[22] S. Henz and J. Herrmann, *Self-channeling and pulse shortening of femtosecond pulses in multiphoton-ionized dispersive dielectric solids*, Phys. Rev. A, 59 (1999), pp. 2528–2531.
[23] V. Karpman and V. Solov'ev, *A perturbational approach to the two-soliton systems*, Phys. D, 3 (1981), pp. 487–502.
[24] T. Kato, *On nonlinear Schrödinger equations*, Ann. Inst. H. Poincaré Phys. Théor., 46 (1987), pp. 113–129.
[25] D. J. Kaup and A. C. Newell, *Solitons as particles, oscillators, and in slowly changing media: A singular perturbation theory*, Proc. R. Soc. Lond. Ser. A Math. Phys. Sci., 361 (1978), pp. 413–446.
[26] J. Keener and D. McLaughlin, *Solitons under perturbations*, Phys. Rev. A, 16 (1977), pp. 777–790.
[27] P. Kelley, *Self-focusing of optical beams*, Phys. Rev. Lett., 15 (1965), pp. 1005–1007.
[28] W. Królikowski and S. A. Holmstrom, *Fusion and birth of spatial solitons upon collision*, Optics Lett., 22 (1997), pp. 369–371.
[29] M. Landman, G. Papanicolaou, C. Sulem, and P. Sulem, *Rate of blowup for solutions of the nonlinear Schrödinger equation at critical dimension*, Phys. Rev. A, 38 (1988), pp. 3837–3843.
[30] B. LeMesurier, G. Papanicolaou, C. Sulem, and P. Sulem, *Local structure of the self-focusing singularity of the nonlinear Schrödinger equation*, Phys. D, 32 (1988), pp. 210–226.
[31] P. M. Lushnikov, S. A. Dyachenko, and N. Vladimirova, *Beyond leading-order logarithmic scaling in the catastrophic self-focusing of a laser beam in Kerr media*, Phys. Rev. A, 88 (2013), 013845.

[32] G. Luther, A. Newell, and J. Moloney, *The effects of normal dispersion on collapse events*, Phys. D, 74 (1994), pp. 59–73.
[33] V. Malkin, *On the analytical theory for stationary self-focusing of radiation*, Phys. D, 64 (1993), pp. 251–266.
[34] F. Merle, *Limit behavior of saturated approximations of nonlinear Schrödinger equation*, Comm. Math. Phys., 149 (1992), pp. 377–414.
[35] F. Merle, *On uniqueness and continuation properties after blow-up time of self-similar solutions of nonlinear Schrödinger equation with critical exponent and critical mass*, Comm. Pure Appl. Math., 45 (1992), pp. 203–254.
[36] F. Merle and P. Raphael, *On a sharp lower bound on the blow-up rate for the L^2 critical nonlinear Schrödinger equation*, J. Amer. Math. Soc., 19 (2006), pp. 37–90.
[37] R. L. Pego and M. I. Weinstein, *Eigenvalues, and instabilities of solitary waves*, Philos. Trans. Roy. Soc. London Ser. A, 340 (1992), pp. 47–94.
[38] D. E. Pelinovsky, Y. S. Kivshar, and V. V. Afanasjev, *Internal modes of envelope solitons*, Phys. D, 116 (1998), pp. 121–142.
[39] P. Polynkin, M. Kolesik, E. M. Wright, and J. V. Moloney, *Experimental tests of the new paradigm for laser filamentation in gases*, Phys. Rev. Lett., 106 (2011), 153902.
[40] C. Rotschild, B. Alfassi, O. Cohen, and M. Segev, *Long-range interactions between optical solitons*, Nature Phys., 2 (2006), pp. 769–774.
[41] J. Sanz-Serna and J. Verwer, *Conservative and nonconservative schemes for the solution of the nonlinear Schrödinger equation*, IMA J. Numer. Anal., 6 (1986), pp. 25–42.
[42] A. Shabat and V. Zakharov, *Exact theory of two-dimensional self-focusing and one-dimensional self-modulation of waves in nonlinear media*, Soviet Phys. JETP, 34 (1972), pp. 62–69.
[43] M.-F. Shih and M. Segev, *Incoherent collisions between two-dimensional bright steady-state photorefractive spatial screening solitons*, Optics Lett., 21 (1996), pp. 1538–1540.
[44] S. Skupin, L. Bergé, U. Peschel, F. Lederer, G. Méjean, J. Yu, J. Kasparian, E. Salmon, J. P. Wolf, M. Rodriguez, L. Wöste, R. Bourayou, and R. Sauerbrey, *Filamentation of femtosecond light pulses in the air: Turbulent cells versus long-range clusters*, Phys. Rev. E, 70 (2004), 046602.
[45] C. Sulem and P. Sulem, *The Nonlinear Schrödinger Equation: Self-Focusing and Wave Collapse*, Appl. Math. Sci. 139, Springer-Verlag, New York, 1999.
[46] T. Tao, *Why are solitons stable?*, Bull. Amer. Math. Soc., 46 (2009), pp. 1–33.
[47] N. Vakhitov and A. Kolokolov, *Stationary solutions of the wave equation in a medium with nonlinearity saturation*, Radiophys. and Quantum Electronics, 16 (1973), pp. 783–789.
[48] S. Vlasov, V. Petrishchev, and V. Talanov, *Averaged description of wave beams in linear and nonlinear media (the method of moments)*, Radiophys. and Quantum Electronics, 14 (1971), pp. 1062–1070.
[49] H. Wang, C. Fan, P. Zhang, C. Qiao, J. Zhang, and H. Ma, *Dynamics of femtosecond filamentation with higher-order Kerr response*, J. Opt. Soc. Amer. B, 28 (2011), pp. 2081–2086.
[50] M. J. Ward, W. D. Henshaw, and J. B. Keller, *Summing logarithmic expansions for singularly perturbed eigenvalue problems*, SIAM J. Appl. Math., 53 (1993), pp. 799–828.
[51] M. I. Weinstein, *Modulational stability of ground states of nonlinear Schrödinger equations*, SIAM J. Math. Anal., 16 (1985), pp. 472–491.
[52] T.-T. Xi, X. Lu, Z.-Q. Hao, Y.-Y. Ma, and J. Zhang, *Classical areas of phenomenology: Interaction of light filaments in air*, Chinese Phys. B, 18 (2009), pp. 4303–4307.
[53] V. Zakharov and A. Rubenchik, *Instability of waveguides and solitons in nonlinear media*, Zh. Eksp. Teor. Fiz., 65 (1973), pp. 997–1011.
[54] V. E. Zakharov, *Collapse of Langmuir waves*, Soviet Phys. JETP, 35 (1972), pp. 908–914.